



SkelMamba: A State Space Model for Efficient Skeleton Action Recognition of Neurological Disorders



Niki Martinel
University of Udine

niki.martinel@uniud.it

Mariano Serrao
Sapienza Università di Roma

mariano.serrao@uniroma1.it

Christian Micheloni
University of Udine

christian.micheloni@uniud.it

Abstract

We introduce a novel state-space model (SSM)-based framework for skeleton-based human action recognition, with an anatomically-guided architecture that improves state-of-the-art performance in both clinical diagnostics and general action recognition tasks. Our approach decomposes skeletal motion analysis into spatial, temporal, and spatio-temporal streams, using channel partitioning to capture distinct movement characteristics efficiently. By implementing a structured, multi-directional scanning strategy within SSMs, our model captures local joint interactions and global motion patterns across multiple anatomical body parts. This anatomically-aware decomposition enhances the ability to identify subtle motion patterns critical in medical diagnosis, such as gait anomalies associated with neurological conditions. On public action recognition benchmarks, i.e., NTU RGB+D, NTU RGB+D 120, and NW-UCLA, our model outperforms current state-of-the-art methods, achieving accuracy improvements up to 3.2% with lower computational complexity than previous leading transformer-based models. We also introduce a novel medical dataset for motion-based patient neurological disorder analysis to validate our method’s potential in automated disease diagnosis.

herently challenging. In the medical domain, precisely capturing the dynamic spatio-temporal relationships between joints is of paramount importance for precise analysis of subtle movements indicative of various diseases. For example, analyzing a patient’s gait can provide insights into neurological disorders, musculoskeletal abnormalities, and other health conditions.

The skeleton joints and their connections (i.e., bones) correspond to the vertices and edges of a graph structure. Our community has recently proposed skeleton action recognition methods that model the spatial and temporal dependencies among skeletal joints via Graph Convolution Networks (GCN) or transformer-like architectures. GCN-based methods introduced adaptive graph structures (e.g., [9, 48, 49]), specialized joint encodings (e.g., [4, 32]), and explored multiple modalities (e.g., [34]) for learning robust representations (e.g., [24, 32, 74]). Transformer-based methods tackle the long-range dependencies in skeletal data that GCN-based methods often struggle with. Existing methods model the skeletal spatio-temporal relationship between physically neighboring and distant joints/frames using the self-attention mechanism (e.g., [11, 75]) in one-shot settings (e.g., [77]) or for joint training across different action tasks and datasets (e.g., [14]).

Transformer-like architectures are computationally demanding and GCN-based methods struggle to model the relation of physically distant joints –captured through the direct propagation of information between physically connected joints. This motivates the introduction of our novel state-space model (SSM)-based architecture, which models all joint relationships with an efficient spatial-temporal scanning strategy –designed to analyze skeletal data for patient disease recognition.

Our novel approach introduces a structured decomposition of skeletal motion data operating across three complementary dimensions. Given an input sequence, we first partition its channel representations into specialized groups for spatial, temporal, and spatio-temporal analysis. The spatial and temporal streams capture local patterns and short-range frame-wise transitions, while the spatio-temporal stream in-

1. Introduction

Human action recognition is the task of classifying actions based on human movements. The problem is often tackled by leveraging the rich contextual features in RGB videos –at the cost of exposing information about people’s identities. Skeleton-based action recognition has emerged as a privacy-preserving alternative for sensitive applications, from patient monitoring and physical therapy to assisted living environments.

Skeletal 3D joint representations are compact and robust to environmental conditions (e.g., background clutter and light variations) yet their sparse nature makes this task in-

roduces State Space Models (SSMs) for complex motion modeling.

Neurological disorders impact distinct body parts during locomotion, resulting in disease-specific motion patterns. Within the spatio-temporal stream, we further partition the input according to anatomically meaningful body parts (*e.g.*, legs, torso, arms) and their key interactions (*e.g.*, arms-legs coordination) that are analyzed by separate SSMs. Each SSM features our novel four-way scanning strategy that splits each anatomical group into four channel subgroups. A specific scanning direction is applied to a specific subgroup. This enables efficient parallel processing –while reducing the computational demands of our model– and allows us to collectively analyze the motion patterns across both space and time: from temporal to spatial domain, spatial to temporal domain, and their respective inverse directions. This multi-directional scanning enables comprehensive capture of both local joint relationships and global motion patterns while being computationally efficient.

This new anatomically-aware architecture proves particularly effective for automated medical diagnosis, where subtle motion abnormalities often manifest through complex interactions between different body parts over time. Nevertheless, our model remains generic and demonstrates significant improvements over state-of-the-art results on existing challenging action recognition datasets, showcasing its versatility and robustness.

Our contribution is threefold:

- We propose a novel multi-stream architecture leveraging SSMs that effectively decomposes motion analysis into spatial, temporal, and spatio-temporal streams through channel partitioning, enabling efficient parallel processing of distinct motion characteristics.
- We introduce an anatomically-aware partitioning scheme that guides the SSM analysis based on meaningful body parts and their interactions, capturing both local joint dynamics and complex cross-body motion patterns crucial for medical diagnosis.
- We develop a channel-split scanning mechanism where input features are partitioned into four subgroups, each processed by direction-specific SSMs. This approach enables comprehensive multi-directional motion analysis while maintaining computational efficiency through reduced channel dimensionality.

Through extensive experiments on both medical diagnosis tasks (we introduce a dataset for the analysis of patient walking styles to assist in automated neurological disease diagnosis) and standard action recognition benchmarks, we demonstrate that our method achieves state-of-the-art performance while being very computationally efficient.

2. Related Work

Graph Convolutional Networks (GCNs) have been initially explored for skeleton-based action recognition in [65]. The seminal work introduced the Spatial-Temporal Graph Convolutional Network (ST-GCN) framework for modeling human joints with spatiotemporal graph structures. Recent architectural innovations have evolved along multiple dimensions, from joint-bone fusion networks [43] and multi-scale feature extraction [51] to adaptive graph topology learning [48]. Context-aware architectures [7, 71] and dual-stream temporal models [50] have enhanced feature extraction capabilities, while adaptive graph structures [37, 67] and efficient convolutions [8, 12] have optimized computational overhead. These developments, complemented by multi-modal integration approaches [34], have significantly advanced the field’s ability to capture rich motion characteristics while maintaining robustness across varying conditions.

GCN-based approaches rely on local graph operations and predefined adjacency matrices, limiting their ability to capture long-range dependencies and dynamic motion patterns. Our approach diverges by introducing state-space models (SSMs) for dynamic latent space partitioning, efficiently capturing local and global interactions.

Transformers are a powerful alternative architecture for skeleton-based action recognition, primarily due to their capacity to model complex joints and temporal motion patterns through the self-attention mechanism [55]. Spatial-temporal attention frameworks [14, 44] enable joint modeling of structural and dynamic information, while global-local attention mechanisms [26] selectively focus on key motion patterns across different temporal scales. Frequency-aware architectures [61] improve data efficiency through spectral augmentation, while specialized designs [11] optimize performance for specific motion types. Multi-modal approaches [57] incorporate complementary sensor data to enhance robustness across varying conditions. Self-supervised pretraining strategies [75] leverage unlabeled data for improved representation learning, while efficient architectural designs [40, 41] maintain high accuracy with reduced computational demands.

Despite these advances, transformer-based methods face inherent limitations due to their quadratic computational complexity in modeling pairwise attention, motivating our exploration of more efficient architectures for real-time applications.

State-space models (SSMs) offer an efficient approach to sequence modeling with long-range dependencies. Initial work on linear state-space layers [18] laid the foundation for S4 [19], while subsequent variants [22, 23, 53] demonstrated comparable performance with simplified architectures. Mamba [17] addressed content-based reasoning limitations through input-dependent parameters [16]. For vi-

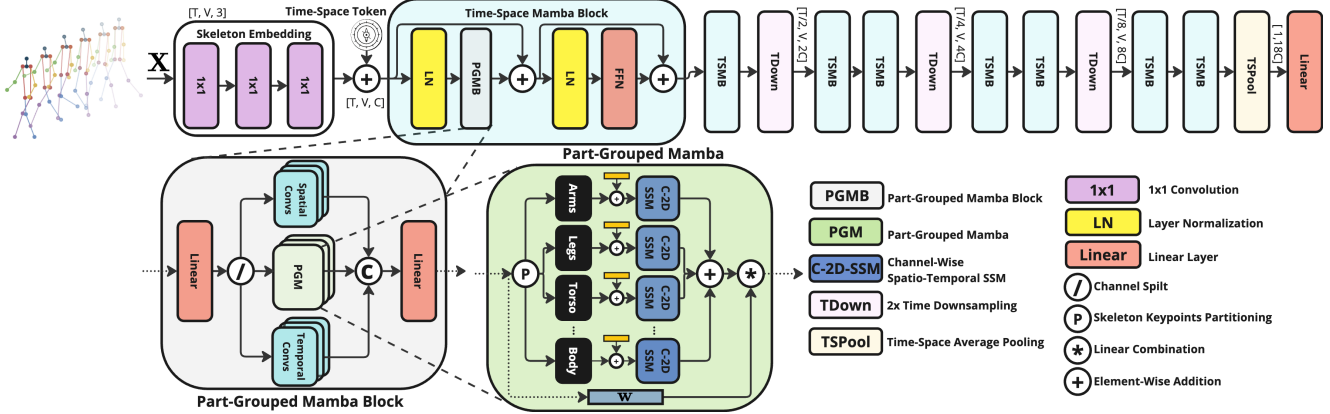


Figure 1. The overall framework of our proposed SkelMamba architecture.

sion tasks, existing SSM adaptations [2, 35, 39, 42] primarily follow fixed unidirectional scanning patterns. Video-based methods [6, 66, 73] process temporal information sequentially after spatial encoding, while 3D approaches [31, 47, 68] rely on predetermined serialization strategies. Recent works have further expanded SSMs to image restoration [10] and speech processing [30], with surveys [64] providing comprehensive overviews.

While SSMs offer flexibility, their adaptation to skeleton-based action recognition remains challenging. The recent work in [5] addressed the problem with a temporal-driven one-direction scanning strategy applied on the top of GCN latent space embeddings. In contrast, we enable simultaneous four-way scanning (spatial-temporal, temporal-spatial, in both forward/backward directions) through channel grouping. Experimental comparisons show that this efficient multi-directional processing captures richer motion dependencies yielding improved skeleton-based analysis.

Automated diagnosis of neurological disorders has made significant progress through multi-modal approaches and advanced architectures. Recent methods have demonstrated success by integrating skeleton data with foot pressure information for Parkinson’s Disease (PD) assessment [38], while graph-based networks enhanced with causality mechanisms have improved Freezing of Gait detection [20]. Clinical findings have shown that fine-tuned motion encoders effectively capture pathological gait patterns [1], complemented by spatiotemporal architectures for PD recognition [69]. Vision-based ensemble discriminate between PD and knee osteoarthritis gaits [27], building upon established clinical characterizations of disorder-specific gait patterns [15, 45]. More recently, transformer architectures have demonstrated promising results in early PD detection [36]. These advances underscore the growing potential of computer vision for objective clinical gait assessment [21].

These existing approaches often hinge on complex pre-

processing/modeling architecture or raise privacy concerns through video analysis. Our model operates directly on skeletal data and captures distinct spatiotemporal dynamics in walking patterns without requiring extensive computational resources or compromising patient privacy, advancing the state-of-the-art in skeleton-based action recognition.

3. SkelMamba

The SkelMamba architecture is illustrated in Figure 1. A skeleton sequence is denoted as $\mathbf{X} \in \mathbb{R}^{T \times V \times C}$, where T is the sequence length, V is the number of joints per frame, and C represents the joint coordinates.

Three linear layers project the low-dimensional skeleton data onto a higher-dimensional embedding space. A learnable time-space token is added to the embedding, then input to L Time-Space Mamba Blocks (TSMB), each containing a Part-Group Mamba Block (PGMB) modeling the skeletal-temporal relations and a feed-forward network (FFN) for feature refinement. To retain temporal dynamics information while reducing the computational complexity, after two TSMB blocks, a TDown layer consisting of a Conv1D with a stride of 2 followed by BN is applied. The features obtained after the L TSMBs undergo skeletal-temporal average pooling followed by a Linear layer producing $\hat{\mathbf{y}} \in \mathbb{R}^C$, with C denoting the number of classes.

3.1. Time-Space Mamba Block (TSMB)

To design our novel TSMB, we follow a similar structure to traditional transformer blocks [55]. The first part of the block models the spatial-temporal dynamics via part-grouped interactions

$$\mathbf{X} = \mathbf{X} + \text{PGMB}(\text{LN}(\mathbf{X})) \quad (1)$$

with the PGMB block computing

$$[\mathbf{X}_s, \mathbf{X}_m, \mathbf{X}_t] = \text{Split}(\text{Linear}(\mathbf{X})) \quad (2)$$

$$\mathbf{X}_s = \text{SpatialConv}(\mathbf{X}_s) \quad (3)$$

$$\mathbf{X}_m = \text{PGM}(\mathbf{X}_m) \quad (4)$$

$$\mathbf{X}_t = \text{TemporalConv}(\mathbf{X}_t) \quad (5)$$

$$\mathbf{X} = \text{Linear}(\text{Concat}(\mathbf{X}_s, \mathbf{X}_m, \mathbf{X}_t)) \quad (6)$$

where LN is the Layer Normalization operator, and Split and Concat are the channel splitting and concatenation functions. For input \mathbf{X} , we split it into \mathbf{X}_s , \mathbf{X}_m , and \mathbf{X}_t with $C/4$, $C/2$, and $C/4$ channels, respectively.

Following a similar spirit to multi-head attention mechanisms, we have $H/4$ parallel PGM, SpatialConv, and TemporalConv operators, with H denoting the number of heads. The novel PGM layer models spatial-temporal relationships of different body parts in \mathbf{X}_m . Each SpatialConv is a one-layer GCN with a learnable $(H/4, V, V)$ matrix –instead of a predefined adjacency matrix– that captures diverse joint spatial connectivity patterns in \mathbf{X}_s . To model temporal dynamics of patterns in \mathbf{X}_t , every TemporalConv performs a $H/4$ -grouped Conv1D filtering operation, with kernel size k_t .

The second part of the block refines the captured skeletal spatial-temporal dynamics by computing

$$\mathbf{X} = \mathbf{X} + \underbrace{\text{Linear}(\text{GELU}(\text{Linear}(\text{LN}(\mathbf{X}))))}_{\text{FFN}} \quad (7)$$

which corresponds to the output of a TSMB.

3.2. Part-Grouped Mamba (PGM)

This layer is designed following three key insights: (i) spatial (SpatialConv) and temporal (TemporalConv) operators model short-range temporal dynamics of the whole body; (ii) different diseases affect specific body parts which exhibit distinct yet interrelated long-range temporal dynamics. Following such intuitions, our novel PGM introduces channel-wise driven scanning and part-based decomposition strategies in State Space Models [19] to efficiently capture long-range local and global motion patterns.

State Space Models (SSMs) are designed to map a 1D input sequence $x(t) \in \mathbb{R}$ to an output $y(t) \in \mathbb{R}$ using a hidden state $\mathbf{h}(t) \in \mathbb{R}^N$. Formally, this mapping is governed by the following ordinary differential equations (ODEs):

$$\begin{aligned} \mathbf{h}'(t) &= \mathbf{A}\mathbf{h}(t) + \mathbf{B}x(t) \\ y(t) &= \mathbf{C}\mathbf{h}(t) \end{aligned} \quad (8)$$

where $\mathbf{A} \in \mathbb{R}^{N \times N}$ is the system's evolution matrix, and $\mathbf{B} \in \mathbb{R}^{N \times 1}$, $\mathbf{C} \in \mathbb{R}^{1 \times N}$ are projection matrices. Modern SSMs [19] discretize (8) using the zero-order hold (ZOH) method

$$\begin{aligned} \bar{\mathbf{A}} &= \exp(\Delta\mathbf{A}) \\ \bar{\mathbf{B}} &= (\Delta\mathbf{A})^{-1}(\exp(\Delta\mathbf{A}) - \mathbf{I}) \cdot \Delta\mathbf{B} \end{aligned} \quad (9)$$

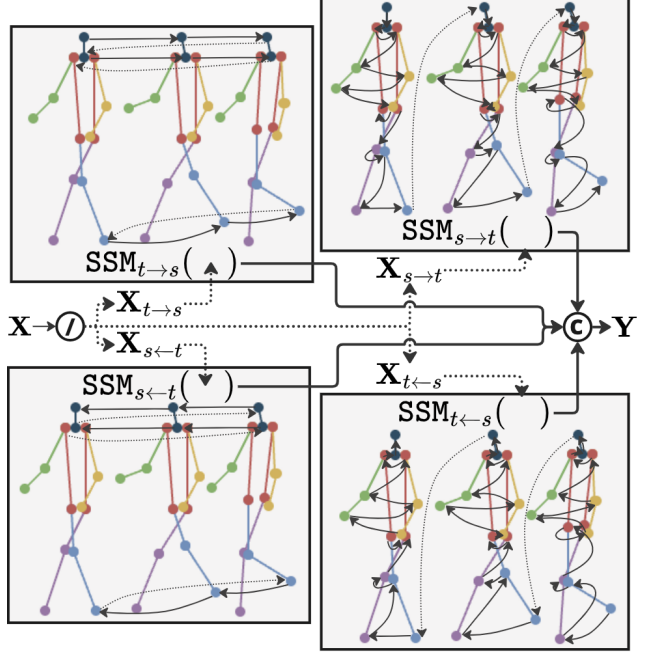


Figure 2. Channel-Wise Spatio-Temporal SSM (C-2D-SSM).

with timescale parameter Δ –which can be seen as the resolution of the continuous input $x(t)$ – leading to the discrete state-space equations

$$\begin{aligned} \mathbf{h}_t &= \bar{\mathbf{A}}\mathbf{h}_{t-1} + \bar{\mathbf{B}}x_t \\ y_t &= \mathbf{C}\mathbf{h}_t \end{aligned} \quad (10)$$

that can be efficiently computed by the convolution

$$\begin{aligned} \bar{\mathbf{K}} &= (\mathbf{C}\bar{\mathbf{B}}, \mathbf{C}\bar{\mathbf{A}}\bar{\mathbf{B}}, \dots, \mathbf{C}\bar{\mathbf{A}}^{L-1}\bar{\mathbf{B}}) \\ y &= \mathbf{x} * \bar{\mathbf{K}} \end{aligned} \quad (11)$$

where L denotes the length of the input sequence \mathbf{x} and $\bar{\mathbf{K}}$ is the SSM convolutional kernel.

Unlike traditional linear time-invariant SSMs, Mamba [17] introduces a Selective Scan Mechanism (S6) such that parameters \mathbf{B} , \mathbf{C} , and Δ are directly derived from the input data, hence allowing input-dependent interactions along the sequence.

Channel-Wise Spatio-Temporal SSM (C-2D-SSM): The Mamba architecture has been extended from 1D to 2D bidirectional modeling (e.g., [2, 35, 64]) showing promise in image-related tasks but exhibiting instability when scaled to large parameter spaces [42]. This is due to the Mamba block's extensive input and output projections, whose computational and parametric complexities scale linearly with the input channel dimensionality.

To effectively mitigate these issues, we leverage the insight that different channel groups in skeletal data may represent distinct yet complementary aspects of movement. As

shown in Figure 2, we decompose the input \mathbf{X} along the channel dimension to get equally sized tensors

$$[\mathbf{X}_{t \rightarrow s}, \mathbf{X}_{s \rightarrow t}, \mathbf{X}_{t \leftarrow s}, \mathbf{X}_{s \leftarrow t}] = \text{Split}(\mathbf{X}) \quad (12)$$

that are independently processed by direction-specific 2D-SSMs (*i.e.*, spatial-temporal SSMs), then concatenated back to produce the final output

$$\mathbf{Y} = \text{Concat} \begin{pmatrix} \text{SSM}_{t \rightarrow s}(\mathbf{X}_{t \rightarrow s}), \\ \text{SSM}_{s \rightarrow t}(\mathbf{X}_{s \rightarrow t}), \\ \text{SSM}_{t \leftarrow s}(\mathbf{X}_{t \leftarrow s}), \\ \text{SSM}_{s \leftarrow t}(\mathbf{X}_{s \leftarrow t}) \end{pmatrix} = \text{C2DSSM}(\mathbf{X}) \quad (13)$$

preserving the input tensor’s dimensionality. t and s denote temporal and spatial dimensions, respectively, and the arrows indicate the direction of spatial-temporal scanning.

This novel parallel approach captures complementary movement features across channel groups, while significantly reducing the computational complexity by operating on $C/4$ channel inputs. The direction-specific spatial-temporal scanning mechanism effectively captures diverse contextual information, enhancing the model’s capacity to learn both local and global dependencies.

Part-Grouped Modeling: Joint locations change over time depending on the disease type. Different deficits are caused by the involvement of multiple systems and structures (*e.g.*, cerebellar, pyramidal, extrapyramidal). For instance, hereditary paraplegia mostly involves lower body part joints [45], while Parkinson’s and Cerebellar Ataxia involve the whole body [15]. Motivated by these intuitions, we introduce both part-based and global SSMs to effectively capture fine-grained local motion details at individual body parts’ level, while maintaining the global understanding of full-body motion.

We decompose the body keypoints into multiple partitions corresponding to key body parts (arms, legs, torso) and their relevant combinations (arms-legs, arms-torso, torso-legs). By focusing on these specific partitions, we enable our model to capture both localized movements and inter-segment temporal dynamics crucial for disease recognition.

For each partition $p \in \{1, \dots, P\}$, we apply:

$$\mathbf{X}_p = \text{C2DSSM}_p(\mathbf{b}_p + \mathbf{X}[:, \mathcal{I}_p]) \quad (14)$$

where \mathcal{I}_p is the index set, $\mathbf{b}_p \in \mathbb{R}^{T \times |\mathcal{I}_p| \times C}$ is a learnable partition token, and C2DSSM_p is our novel C-2D-SSM for partition p .

The learnable partition token \mathbf{b}_p enables each SSM to learn a specialized representation of the motion dynamics specific to each body part or combination, enhancing the model’s ability to differentiate between fine-grained movements. By processing these partitions separately, our model can efficiently capture part-specific temporal patterns, such

as the rhythmic alternation of arm and leg movements during walking, or the stabilizing role of the torso in maintaining balance.

To ensure that full-body motion patterns are not missed when focusing solely on individual parts, we capture holistic motion characteristics as $\mathbf{X}_g = \text{C2DSSM}(\mathbf{X})$.

Attentive SSM: The outputs from these specialized SSMs are then integrated through a learnable weighted sum:

$$\mathbf{X}_{\text{SSM}} = \sum_p \beta_p \mathbf{X}_p + \beta_g \mathbf{X}_g \quad (15)$$

where β_p and β_g are learnable parameters. This integration strategy allows our model to dynamically adjust the importance of part-specific and global motion information based on the input data.

To further refine our feature representations and enhance the model’s adaptability, we incorporate a channel attention mechanism after the SSM processing. We first compute

$$\mathbf{w} = \sigma(\text{Linear}(\text{GELU}(\text{Linear}(\text{Pool}(\mathbf{X}_{\text{SSM}})))))) \quad (16)$$

where Pool is the spatial-temporal average pooling operator and σ is the sigmoid function. Then, we obtain the output of our novel PGM as

$$\text{PGM}(\mathbf{X}) = (\mathbf{X}_{\text{SSM}} + \mathbf{X}) \odot \mathbf{w} \quad (17)$$

where α is a learnable parameter and \odot denotes the Hadamard product. The residual connection ($+\mathbf{X}$) ensures efficient gradient flow during training, while the channel attention ($\odot \mathbf{w}$) allows our model to adaptively recalibrate channel-wise feature responses [25], focusing on the most informative features for each input sequence.

4. Experiments

4.1. Datasets

Medical Diagnosis: Our objective is to provide a method for automated diagnosis of motion-related disorders. To assess the capabilities of our method in such a context, we validate it on one newly collected dataset and a publicly available benchmark. Both datasets present a challenging scenario for automated diagnosis from skeleton action recognition, requiring models to differentiate between multiple neurological conditions and healthy controls based on subtle motion characteristics.

Neurological Disorders (ND). We collected a new dataset focused on automated diagnosis of neurological disorders. Our dataset comprises 396 video sequences from 40 subjects across four distinct classes: primary degenerative cerebellar ataxia (11 patients, 112 sequences), hereditary spastic paraparesis (12 patients, 105 sequences), idiopathic Parkinson’s disease (7 patients, 80 sequences), and healthy controls (10 subjects, 99 sequences). Data collection was

Table 1. Comparison with existing methods on the three considered medical diagnosis benchmark datasets: ND, KOA-PD-NM (3 classes with grouped severity levels), and KOA-PD-NM-Severity (7 classes with different diseases’ severity levels). Results are shown considering the number of input frames and ensemble strategies.

Type	Model	ND			KOA-PD-NM			KOA-PD-NM-Severity		
		\mathbb{M}_j	\mathbb{M}_{jb}	\mathbb{M}_{jbm}	\mathbb{M}_j	\mathbb{M}_{jb}	\mathbb{M}_{jbm}	\mathbb{M}_j	\mathbb{M}_{jb}	\mathbb{M}_{jbm}
CNN	PoseC3D [13]	98.95	99.21	99.35	84.79	89.40	89.86	95.79	98.95	98.95
GCN	2S-AAGCN [48]	94.74	97.89	98.95	91.22	92.39	93.18	89.47	93.68	93.68
	STGCN++ [65]	93.68	94.74	95.79	93.54	94.31	95.32	95.32	95.79	96.84
Transformer	Hyperformer [75]	99.21	99.35	99.21	96.82	96.94	98.14	95.79	96.84	98.95
SSM	SkelMamba (Ours)	99.35	99.35	99.64	97.45	98.23	98.62	96.84	98.95	99.21

conducted under carefully controlled conditions to ensure consistency and reliability. Each sequence captures a patient walking in a standardized environment, with multiple recordings per subject in both directions - towards and away from the camera. All sequences were recorded using an HD camera operating at 30 fps. The average sequence length is 140.64 frames, with a range from 69 to 465 frames, providing sufficient temporal context for analyzing motion characteristics associated with each condition.

KOA-PD-NM [27] contains marker-based sequences of subjects with Knee Osteoarthritis (KOA, 50 patients), Parkinson’s Disease (PD, 20 patients), and Normal (NM, 30 patients) motion patterns. This dataset was captured in a controlled indoor environment (subjects walked on a green mat in the sagittal plane) using a 50fps HD camera. The dataset includes varying severity levels (mild, moderate, severe) for KOA and PD subjects, graded by medical specialists. We report the results computed considering and excluding the severity levels (*i.e.*, yielding a 7-class and a 3-class dataset, respectively).

Generic Actions: While our approach is primarily designed for automated diagnosis of motion-related neurological disorders, we hypothesize its potential in generic action recognition tasks. To validate this hypothesis and provide a comprehensive evaluation, we conduct experiments on established public benchmarks for skeleton-based action recognition.

NTU RGB+D [46] comprises 60 action classes, encompassing a wide range of daily activities. It contains 56,880 video samples captured from 40 subjects across 155 camera viewpoints using Kinect v2, providing RGB, IR, depth, and 3D skeleton data. The dataset supports cross-subject (X-Sub60) and cross-view (X-View60) evaluation protocols. 11 classes involve two-person interactions, forming the NTU-Inter subset [11, 14, 41].

NTU RGB+D 120 [33] extends the NTU RGB+D dataset to 120 action classes with 114,480 video samples from 106 subjects. It introduces cross-subject (X-Sub120) and cross-setup (X-Set120) evaluation protocols. The dataset includes 26 classes focused on human interaction, designated as NTU-Inter 120 [11, 14, 41].

NW-UCLA [56] consists of 1,475 video samples spanning 10 action classes, performed by 10 subjects and captured from three distinct camera views. It provides RGB, IR, depth, and 3D skeleton data. Evaluation is conducted using a cross-view protocol [11, 75], utilizing two views for training and one for testing.

4.2. Implementation Details

We trained our model on an NVIDIA L40S GPU using the PyTorch framework for 500 epochs on 128-sample batches, using the AdamW optimizer with weight decay equal to $5e-4$. We adopted a linear learning rate warm-up from $1e-7$ to $1e-3$ over the first 25 epochs, followed by a cosine annealing scheduler. We applied clipping for gradients having ℓ_2 -norm exceeding 1. The label-smoothed cross-entropy loss with $\alpha = 0.1$ was used for optimization. For the ND and KOA-PD-NM datasets, we used [54] to obtain the skeleton joints. For others, we used the provided keypoints.

4.3. State-of-the-art Comparison

We present a comprehensive performance comparison of our method against recent state-of-the-art skeleton-based action recognition methods. Following [11, 74, 75], we considered three different modalities: (i) only joints (\mathbb{M}_j) (ii) joints and bones (\mathbb{M}_{jb}); and (iii) joints and bones with motions (\mathbb{M}_{jbm}). We trained a model for each modality and ensemble their outputs.

Medical Diagnosis: Table 1 provides a comparative evaluation of different models on three medical diagnosis datasets. Our proposed model achieves the highest accuracy across all datasets and ensemble metrics. For the ND dataset, we reach 99.35% on \mathbb{M}_j and \mathbb{M}_{jb} , further improving to 99.64% on \mathbb{M}_{jbm} , demonstrating robust performance in diagnosis of neurological disorders.

In the KOA-PD-NM dataset, we significantly improve other methods reading a 98.62% accuracy using the \mathbb{M}_{jbm} . This indicates a strong capability in classifying grouped severity levels. On the more challenging KOA-PD-NM-Severity dataset, our method better handles fine-grained severity distinctions outperforming all existing models.

Table 2. Comparison with existing methods on the three considered generic actions benchmark datasets: NTU RGB+D, NTU RGB+D 120, and NW-UCLA. Results are shown considering the number of input frames and ensemble strategies.

Types	Methods	Frames	NTU RGB+D						NTU RGB+D 120						NW UCLA
			X-Sub60			X-View60			X-Sub120			X-Set120			
			M_j	M_{jb}	M_{jbm}	M_j	M_{jb}	M_{jbm}	M_j	M_{jb}	M_{jbm}	M_j	M_{jb}	M_{jbm}	
RNN	AGC-LSTM [52]	100	87.5	89.2	-	93.5	95.0	-	-	-	-	-	-	-	93.3
CNN	TA-CNN [63]	64	88.8	-	90.4	93.6	-	94.8	82.4	-	85.4	84.0	-	86.8	96.1
	Ske2Grid [3]	100	88.3	-	-	95.7	-	-	82.7	-	-	85.1	-	-	-
GCN	SGN [70]	20	-	89.0	-	-	94.5	-	79.2	-	-	81.5	-	-	-
	CTR-GCN [7]	64	89.9	-	92.4	-	-	96.8	84.9	88.7	88.9	-	90.1	90.6	96.5
	ST-GCN++ [65]	100	89.3	91.4	92.1	95.6	96.7	97.0	83.2	87.0	87.5	85.6	87.5	89.8	-
	InfoGCN [9]	64	-	-	92.7	-	-	96.9	85.1	88.5	89.4	86.3	89.7	90.7	96.6
	FR-Head [74]	64	90.3	92.3	92.8	95.3	96.4	96.8	85.5	-	89.5	87.3	-	90.9	96.8
	Koopman [59]	64	90.2	-	92.9	95.2	-	96.8	85.7	-	90.0	87.4	-	91.3	97.0
	LST [62]	64	90.2	-	92.9	95.6	-	97.0	85.5	-	89.9	87.0	-	91.1	97.2
	HD-GCN [29]	64	90.6	92.4	93.0	95.7	96.6	97.0	85.7	89.1	89.8	87.3	90.6	91.2	96.9
	STC-Net [28]	64	-	92.5	93.0	-	96.7	97.1	-	89.3	89.9	-	90.7	91.3	97.2
	BlockGCN [76]	64	90.9	-	93.1	95.4	-	97.0	86.9	-	90.3	88.2	-	91.5	96.9
	DSTA-Net [50]	128	-	-	91.5	-	-	96.4	-	-	86.6	-	-	89.0	-
Transf.	STST [72]	128	-	-	91.9	-	-	96.8	-	-	-	-	-	-	-
	FG-STFormer [58]	128	-	-	92.6	-	-	96.7	-	-	89.0	-	-	90.6	97.0
	Hyperformer [75]	64	90.7	-	92.9	95.1	-	96.5	86.6	-	88.0	88.0	-	91.3	96.7
CCM	Simba [42]	64	89.0	90.5	-	94.4	95.2	-	79.7	-	-	86.3	-	-	96.3
	SkelMamba (Ours)	64	91.8	92.8	93.4	96.8	97.1	97.4	87.1	89.4	89.9	89.1	90.7	91.5	97.6

Table 3. Comparison with existing human interaction recognition methods on the NTU-Inter and NTU-Inter 120 datasets.

Types	Methods	NTU-Inter (M_j , %)		NTU-Inter 120 (M_j , %)		Params [M]	FLOPs [G]	Time [ms]
		X-Sub60	X-View60	X-Sub120	X-Set120			
Transformer	IGFormer [41]	93.6	96.5	85.4	86.5	-	-	-
	SkeleTR [14]	94.9	97.7	87.8	88.3	3.82	7.30	-
	ISTA-Net [60]	-	-	90.6	91.7	6.22	68.18	21.71
SSM	SkelMamba (Ours)	96.5	98.9	92.0	92.8	6.84	9.7	7.06

Our novel state-space model architecture achieves substantial performance gains across datasets, highlighting its effectiveness for nuanced medical diagnosis tasks that require precise classification of disease severity. This is likely due to the model’s ability to dynamically capture long-range local and global joint interactions.

Generic Actions: Results in Table 2 show that our noble method achieves leading performance across diverse generic action recognition benchmarks. We consistently outperformed prior methods, demonstrating the effectiveness of our modeling approach. On the NTU RGB+D X-Sub60 dataset, we recorded top scores of 91.8%, 92.8%, and 93.4% across the three considered ensemble strategies, showing the capabilities of our approach in capturing spatial-temporal dependencies. For the more complex NTU RGB+D 120 dataset, our method demonstrates excellent performance by improving over prior GCN and Transformer-based methods. Similarly, on the NW-UCLA dataset, we obtain the highest accuracy at 97.6% on the leaderboard.

Similar comments can be made for the results obtained comparing our method with state-of-the-art human interac-

tion recognition methods on the NTU-inter and NTU-Inter 120 datasets. Table 3 shows that we consistently achieve superior performance than existing methods, demonstrating the robustness and effectiveness of our approach in handling complex human interactions.

Complexity Analysis: Table 4 provides a comparative computational complexity analysis with existing architectures. Our approach achieves the highest accuracy, recording an average joint modality accuracy of 94.3% and 88.1% on the NTU RGB+D and NTU RGB+D 120 datasets respectively –surpassing all existing methods. While SkelMamba exhibits a slightly higher parameter count (6.84M) and FLOPs (9.7G) than some lighter GCN models, its inference time of 7.06 ms shows it is remarkably efficient. This trade-off positions our method as the most accurate and fastest model.

4.4. Ablation Study

Part-Grouped Mamba Block Components: Table 5 presents an ablation study on the novel part-grouped mamba block, investigating the contributions of its spatial, temporal, and spatio-temporal components. The ablation of either

Table 4. Computational analysis: comparison of parameters, FLOPs, inference time, and average top-1 accuracy for joint modality (\uparrow higher is better, \downarrow lower is better).

Types	Methods	Params [M] \downarrow	FLOPs [G] \downarrow	Time [ms] \downarrow	NTU RGB+D [%] \uparrow	NTU RGB+D 120 [%] \uparrow
GCN	InfoGCN [9]	1.56	3.34	12.97	-	85.7
	FR-Head [74]	1.45	3.60	18.49	92.8	86.4
	Koopman [59]	5.38	8.76	17.86	92.7	86.6
	LST [62]	2.10	3.60	18.85	92.9	86.3
	HD-GCN [29]	1.66	3.44	72.81	93.2	86.5
Transformer	DSTA-Net [50]	3.45	16.18	13.80	-	-
	Hyperformer [75]	2.71	9.64	18.07	92.9	87.3
SSM	SkelMamba (Ours)	6.84	9.7	7.06	94.3	88.1

Table 5. Ablation analysis of the spatial, temporal, and spatio-temporal components of the novel part-grouped mamba block. Results show the top-1 accuracy for the \mathbb{M}_j modality (\uparrow higher is better, \downarrow lower is better).

Components			NTU RGB+D [%] \uparrow		Params [M] \downarrow	FLOPs [G] \downarrow	Time [ms] \downarrow
SpatialConv	TemporalConv	PGM	X-Sub60	X-View60			
\checkmark			89.9	94.6	4.3	8.2	2.65
	\checkmark		87.2	93.5	4.1	8.1	1.80
		\checkmark	90.9	95.1	6.6	9.5	6.90
\checkmark	\checkmark		90.6	94.8	4.3	8.2	2.99
\checkmark		\checkmark	91.0	95.8	6.7	9.4	3.85
	\checkmark	\checkmark	91.1	95.4	6.6	9.4	5.76
\checkmark	\checkmark	\checkmark	91.8	96.8	6.8	9.7	7.06

Table 6. Contribution of the introduced components of the novel part grouped mamba (PGM) layer. Results show the top-1 accuracy for the \mathbb{M}_j modality.

PGM	NTU RGB+D [%]	
	X-Sub60	X-View60
1D SSM Baseline	88.6	94.1
+ 1D SSM to C-2D-SSM	90.2 (+1.6)	95.3 (+1.2)
+ Partition Token (\mathbf{b}_p)	90.5 (+0.3)	95.6 (+0.3)
+ Attentive SSM (\mathbf{X}_{SSM})	91.6 (+1.1)	96.4 (+0.8)
+ Channel attention (\mathbf{w})	91.8 (+0.7)	96.8 (+0.4)

the spatial or temporal component leads to a significant drop in accuracy, highlighting the importance of both modalities for the block’s performance. The PGM module, which models interactions of different parts of the body, consistently improves accuracy across all configurations. This suggests that the PGM effectively captures the spatial relationships between body parts.

Body partitioning and SSM scanning: Table 6 presents the ablation study of the Part Grouped Mamba (PGM) layer. Transitioning from 1D SSM to C-2D-SSM notably improves performance, highlighting the benefit of spatial-temporal dependency modeling. Incorporating attentive SSM enhances performance by capturing long-range dependencies, while channel attention refines feature representation, yielding additional gains. Altogether, the fully integrated PGM layer achieves the highest accuracy,

validating its design for robust part-based skeleton action recognition.

5. Conclusion

We presented a novel skeleton-based action recognition framework that integrates anatomically-aware State Space Models (SSMs) for fine-grained analysis of spatio-temporal motion patterns. Our approach introduces a multi-stream architecture that partitions skeletal data into spatial, temporal, and spatio-temporal streams, enabling efficient and targeted analysis of complex human motions. Through anatomically-guided body part segmentation and a multi-directional scanning strategy, our method captures both local joint dynamics and global motion interactions crucial for applications requiring precision, such as automated medical diagnosis.

Extensive evaluations on standard benchmarks (NTU RGB+D, NTU RGB+D 120, NW-UCLA) demonstrate our model’s superiority by significantly improving over existing methods. On a new medical dataset for gait analysis, our framework also exhibits strong potential for clinical diagnostics, accurately identifying subtle movement patterns indicative of neurological disorders. However, our medical dataset remains limited in size, as expanding it requires complex data-gathering processes constrained by privacy concerns and regulatory restrictions. We are actively working to increase this dataset, but this endeavor remains resource-intensive.

References

- [1] Vida Adeli, Soroush Mehraban, Irene Ballester, Yasamin Zarghami, Andrea Sabo, Andrea Iaboni, and Babak Taati. Benchmarking skeleton-based motion encoder models for clinical applications: Estimating parkinson’s disease severity in walking sequences, 2024. [3](#)
- [2] Anwai Archit and Constantin Pape. Vim-UNET: Vision mamba for biomedical segmentation. In *MIDL*, 2024. [3](#), [4](#)
- [3] Dongqi Cai, Yangyuxuan Kang, Anbang Yao, and Yurong Chen. Ske2grid: Skeleton-to-grid representation learning for action recognition. In *International Conference on Machine Learning*, 2023. [7](#)
- [4] Jinmiao Cai, Nianjuan Jiang, Xiaoguang Han, Kui Jia, and Jiangbo Lu. Jolo-gcn: Mining joint-centered lightweight information for skeleton-based action recognition. In *IEEE/CVF Winter Applications of Computer Vision*, 2021. [1](#)
- [5] Soumyabrata Chaudhuri and Saumik Bhattacharya. Simba: Mamba augmented u-shifftgcn for skeletal action recognition in videos. *ArXiv Preprint*, 2024. [3](#)
- [6] Guo Chen, Yifei Huang, Jilan Xu, Baoqi Pei, Zhe Chen, Zhiqi Li, Jiahao Wang, Kunchang Li, Tong Lu, and Limin Wang. Video mamba suite: State space model as a versatile alternative for video understanding, 2024. [3](#)
- [7] Yuxin Chen, Ziqi Zhang, Chunfeng Yuan, Bing Li, Ying Deng, and Weiming Hu. Channel-wise topology refinement graph convolution for skeleton-based action recognition. In *International Conference on Computer Vision*, 2021. [2](#), [7](#)
- [8] Ke Cheng, Yifan Zhang, Xiangyu He, Weihan Chen, Jian Cheng, and Hanqing Lu. Skeleton-based action recognition with shift graph convolutional network. In *IEEE/CVF International Conference on Computer Vision and Pattern Recognition*, 2020. [2](#)
- [9] Hyung-Gun Chi, Hoon Ha, Seunggeun Chi, Sang Wan Lee, Qixing Huang, and Karthik Ramani. Infogcn: Representation learning for human skeleton-based action recognition. In *IEEE/CVF International Conference on Computer Vision and Pattern Recognition*, 2022. [1](#), [7](#), [8](#)
- [10] Rui Deng and Tianpei Gu. Cu-mamba: Selective state space models with channel learning for image restoration, 2024. [3](#)
- [11] Jeonghyeok Do and Munchurl Kim. Skateformer: Skeletal-temporal transformer for human action recognition. In *European Conference on Computer Vision*, 2024. [1](#), [2](#), [6](#)
- [12] Haodong Duan, Jiaqi Wang, Kai Chen, and Dahua Lin. Pyskl: Towards good practices for skeleton action recognition. *arXiv preprint arXiv:2205.09443*, 2022. [2](#)
- [13] Haodong Duan, Yue Zhao, Kai Chen, Dahua Lin, and Bo Dai. Revisiting skeleton-based action recognition. In *IEEE/CVF Conference on Computer Vision and Pattern Recognition*, pages 2959–2968. IEEE, 2022. [6](#)
- [14] Haodong Duan, Mingze Xu, Bing Shuai, Davide Modolo, Zhuowen Tu, Joseph Tighe, and Alessandro Bergamo. Skeletr: Towards skeleton-based action recognition in the wild. In *IEEE/CVF International Conference on Computer Vision*, 2023. [1](#), [2](#), [6](#), [7](#)
- [15] G. Ebersbach, M. Sojer, F. Valldeoriola, J. Wissel, J. Müller, E. Tolosa, and W. Poewe. Comparative analysis of gait in Parkinson’s disease, cerebellar ataxia and subcortical arteriosclerotic encephalopathy. *Brain*, 122(7):1349–1355, 1999. [3](#), [5](#)
- [16] Daniel Y. Fu, Tri Dao, Khaled K. Saab, Armin W. Thomas, Atri Rudra, and Christopher Ré. Hungry hungry hippos: Towards language modeling with state space models. *ArXiv Preprint*, 2022. [2](#)
- [17] Albert Gu and Tri Dao. Mamba: Linear-time sequence modeling with selective state spaces. *ArXiv Preprint*, 2023. [2](#), [4](#)
- [18] Albert Gu, Isys Johnson, Karan Goel, Khaled Saab, Tri Dao, Atri Rudra, and Christopher Ré. Combining recurrent, convolutional, and continuous-time models with linear state-space layers. In *Advances in Neural Processing Information Systems*, 2021. [2](#)
- [19] Albert Gu, Karan Goel, and Christopher Ré. Efficiently modeling long sequences with structured state spaces. In *International Conference on Learning Representations*, 2022. [2](#), [4](#)
- [20] Rui Guo, Zheng Xie, Chencheng Zhang, and Xiaohua Qian. Causality-enhanced multiple instance learning with graph convolutional networks for parkinsonian freezing-of-gait assessment. *IEEE Transactions on Image Processing*, 33: 3991–4001, 2024. [3](#)
- [21] Yao Guo, Jianxin Yang, Yuxuan Liu, Xun Chen, and Guangzhong Yang. Detection and assessment of parkinson’s disease based on gait analysis: A survey. *Frontiers in Aging Neuroscience*, 14, 2022. [3](#)
- [22] Ankit Gupta, Albert Gu, and Jonathan Berant. Diagonal state spaces are as effective as structured state spaces. In *Advances in Neural Processing Information Systems*, 2022. [2](#)
- [23] Ramin Hasani, Mathias Lechner, Tsun-Hsuan Wang, Makram Chahine, Alexander Amini, and Daniela Rus. Liquid structural state-space models. In *International Conference on Learning Representations*, 2023. [2](#)
- [24] Zhenyu Hou, Xiao Liu, Yukuo Cen, Yuxiao Dong, Hongxia Yang, Chunjie Wang, and Jie Tang. Graphmae: Self-supervised masked graph autoencoders. In *Proceedings of the ACM SIGKDD International Conference on Knowledge Discovery and Data Mining*, pages 594–604. Association for Computing Machinery, 2022. [1](#)
- [25] Jie Hu, Li Shen, Samuel Albanie, Gang Sun, and Enhua Wu. Squeeze-and-excitation networks. *IEEE Transaction on Pattern Analysis and Machine Intelligence*, 2019. [5](#)
- [26] Boeun Kim, Hyung Jin Chang, Jungho Kim, and Jin Young Choi. Global-local motion transformer for unsupervised skeleton-based action learning. In *European Conference on Computer Vision*, 2022. [2](#)
- [27] Navleen Kour, Sunanda Gupta, and Sakshi Arora. A vision-based hybrid ensemble learning approach for classification of gait disorders. *Multimedia Tools and Applications*, 2024. [3](#), [6](#)
- [28] Jungho Lee, Minhyeok Lee, Suhwan Cho, Sungmin Woo, Sungjun Jang, and Sangyoun Lee. Leveraging spatio-temporal dependency for skeleton-based action recognition. In *IEEE/CVF International Conference on Computer Vision*, pages 10221–10230, 2023. [7](#)

- [29] Jungho Lee, Minhyeok Lee, Dogyoon Lee, and Sangyoun Lee. Hierarchically decomposed graph convolutional networks for skeleton-based action recognition. In *IEEE/CVF International Conference on Computer Vision*, pages 10410–10419, 2023. [7](#), [8](#)
- [30] Kai Li and Guo Chen. Spmamba: State-space model is all you need in speech separation, 2024. [3](#)
- [31] Dingkan Liang, Xin Zhou, Wei Xu, Xingkui Zhu, Zhikang Zou, Xiaoqing Ye, Xiao Tan, and Xiang Bai. Pointmamba: A simple state space model for point cloud analysis, 2024. [3](#)
- [32] Lilang Lin, Jiahang Zhang, and Jiaying Liu. Actionlet-dependent contrastive learning for unsupervised skeleton-based action recognition. In *IEEE/CVF International Conference on Computer Vision and Pattern Recognition*, 2023. [1](#)
- [33] Jun Liu, Amir Shahroudy, Mauricio Perez, Gang Wang, Ling-Yu Duan, and Alex C. Kot. Ntu rgb+d 120: A large-scale benchmark for 3d human activity understanding. *IEEE Transactions on Pattern Analysis and Machine Intelligence*, 42:2684–2701, 2020. [6](#)
- [34] Jinfu Liu, Chen Chen, and Mengyuan Liu. Multi-modality co-learning for efficient skeleton-based action recognition. In *ACM Multimedia*, 2024. [1](#), [2](#)
- [35] Jun Ma, Feifei Li, and Bo Wang. U-mamba: Enhancing long-range dependency for biomedical image segmentation, 2024. [3](#), [4](#)
- [36] Lan Ma, Hua Huo, Wei Liu, Changwei Zhao, Jinxuan Wang, and Ningya Xu. Twin-tower transformer network for skeleton-based parkinson’s disease early detection. *Complex and Intelligent Systems*, 2024. [3](#)
- [37] Woomin Myung, Nan Su, Jing-Hao Xue, and Guijin Wang. Degcn: Deformable graph convolutional networks for skeleton-based action recognition. *IEEE Transactions on Image Processing*, 33:2477–2490, 2024. [2](#)
- [38] Muhammad Tahir Naseem, Haneol Seo, Na-Hyun Kim, and Chan-Su Lee. Pathological gait classification using early and late fusion of foot pressure and skeleton data. *Applied Sciences*, 14:558, 2024. [3](#)
- [39] Eric Nguyen, Karan Goel, Albert Gu, Gordon W Downs, Preey Shah, Tri Dao, Stephen A Baccus, and Christopher Ré. S4nd: Modeling images and videos as multidimensional signals using state spaces. In *Advances in Neural Processing Information Systems*, 2022. [3](#)
- [40] Soroush Oraki, Harry Zhuang, and Jie Liang. Lortsar: Low-rank transformer for skeleton-based action recognition, 2024. [2](#)
- [41] Yunsheng Pang, Qihong Ke, Hossein Rahmani, James Bailey, and Jun Liu. Igformer: Interaction graph transformer for skeleton-based human interaction recognition. In *European Conference on Computer Vision*, 2022. [2](#), [6](#), [7](#)
- [42] Badri N. Patro and Vijay S. Agneeswaran. Simba: Simplified mamba-based architecture for vision and multivariate time series. *ArXiv Preprint*, 2024. [3](#), [4](#), [7](#)
- [43] Wei Peng, Xiaopeng Hong, Haoyu Chen, and Guoying Zhao. Learning graph convolutional network for skeleton-based human action recognition by neural searching. In *Proceedings of the AAAI Conference on Artificial Intelligence*, pages 2669–2676, 2020. [2](#)
- [44] Chiara Plizzari, Marco Cannici, and Matteo Matteucci. Spatial temporal transformer network for skeleton-based action recognition. In *International Conference on Pattern Recognition*, pages 694–701, 2021. [2](#)
- [45] Mariano Serrao, Martina Rinaldi, Alberto Ranavolo, Francesco Lacquaniti, Giovanni Martino, Luca Leonardi, Carmela Conte, Tiwana Varrecchia, Francesco Draicchio, Gianluca Coppola, Carlo Casali, and Francesco Pierelli. Gait patterns in patients with hereditary spastic paraparesis. *PLOS ONE*, 11(10):e0164623, 2016. [3](#), [5](#)
- [46] Amir Shahroudy, Jun Liu, Tian-Tsong Ng, and Gang Wang. Ntu rgb+d: A large scale dataset for 3d human activity analysis. In *IEEE International Conference on Computer Vision and Pattern Recognition*, 2016. [6](#)
- [47] Abdelrahman Shaker, Syed Talal Wasim, Salman Khan, Juergen Gall, and Fahad Shahbaz Khan. Groupmamba: Parameter-efficient and accurate group visual state space model, 2024. [3](#)
- [48] Lei Shi, Yifan Zhang, Jian Cheng, and Hanqing Lu. Two-stream adaptive graph convolutional networks for skeleton-based action recognition. In *IEEE/CVF International Conference on Computer Vision and Pattern Recognition*, 2019. [1](#), [2](#), [6](#)
- [49] Lei Shi, Yifan Zhang, Jian Cheng, and Hanqing Lu. Skeleton-based action recognition with directed graph neural networks. In *IEEE/CVF International Conference on Computer Vision and Pattern Recognition*, 2019. [1](#)
- [50] Lei Shi, Yifan Zhang, Jian Cheng, and Hanqing Lu. Decoupled spatial-temporal attention network for skeleton-based action-gesture recognition. In *Asian Conference on Computer Vision*, pages 38–53, 2020. [2](#), [7](#), [8](#)
- [51] Lei Shi, Yifan Zhang, Jian Cheng, and Hanqing Lu. Skeleton-based action recognition with multi-stream adaptive graph convolutional networks. *IEEE Transactions on Image Processing*, 29:9532–9545, 2020. [2](#)
- [52] Chenyang Si, Wentao Chen, Wei Wang, Liang Wang, and Tieniu Tan. An attention enhanced graph convolutional lstm network for skeleton-based action recognition. In *International Conference on Computer Vision and Pattern Recognition*, 2019. [7](#)
- [53] Jimmy T. H. Smith, Andrew Warrington, and Scott W. Linderman. Simplified state space layers for sequence modeling. In *International Conference on Learning Representations*, 2023. [2](#)
- [54] Ke Sun, Bin Xiao, Dong Liu, and Jingdong Wang. Deep high-resolution representation learning for human pose estimation. In *IEEE/CVF International Conference on Computer Vision and Pattern Recognition*, 2019. [6](#)
- [55] Ashish Vaswani, Noam Shazeer, Niki Parmar, Jakob Uszkoreit, Llion Jones, Aidan N. Gomez, Lukasz Kaiser, and Illia Polosukhin. Attention is all you need. In *Advances in Neural Information Processing Systems*, 2017. [2](#), [3](#)
- [56] Jiang Wang, Xiaohan Nie, Yin Xia, Ying Wu, and Song-Chun Zhu. Cross-view action modeling, learning and recognition. In *IEEE International Conference on Computer Vision and Pattern Recognition*, 2014. [6](#)
- [57] Lei Wang and Piotr Koniusz. 3mformer: Multi-order multi-mode transformer for skeletal action recognition. In

- IEEE/CVF International Conference on Computer Vision and Pattern Recognition*, 2023. 2
- [58] Peitao Wang, Pei Lv, Xiaoheng Jiang, Qidong Liu, Pichao Wang, Mingliang Xu, and Wanqing Li. Focal and global spatial-temporal transformer for skeleton-based action recognition. In *Asian Conference on Computer Vision*, 2022. 7
- [59] Xinghan Wang, Xin Xu, and Yadong Mu. Neural koopman pooling: Control-inspired temporal dynamics encoding for skeleton-based action recognition. In *IEEE Computer Society Conference on Computer Vision and Pattern Recognition*, pages 10597–10607, 2023. 7, 8
- [60] Yuhang Wen, Zixuan Tang, Yunsheng Pang, Beichen Ding, and Mengyuan Liu. Interactive spatiotemporal token attention network for skeleton-based general interactive action recognition. In *IEEE/RSJ International Conference on Intelligent Robots and Systems*, 2023. 7
- [61] Wenhan Wu, Ce Zheng, Zihao Yang, Chen Chen, Srijan Das, and Aidong Lu. Frequency guidance matters: Skeletal action recognition by frequency-aware mixed transformer. In *ACM Multimedia*, 2024. 2
- [62] Wangmeng Xiang, Chao Li, Yuxuan Zhou, Biao Wang, and Lei Zhang. Generative action description prompts for skeleton-based action recognition. In *International Conference on Computer Vision*, pages 10242–10251, 2023. 7, 8
- [63] Kailin Xu, Fanfan Ye, Qiaoyong Zhong, and Di Xie. Topology-aware convolutional neural network for efficient skeleton-based action recognition. In *AAAI Conference on Artificial Intelligence*, 2022. 7
- [64] Rui Xu, Shu Yang, Yihui Wang, Yu Cai, Bo Du, and Hao Chen. Visual mamba: A survey and new outlooks, 2024. 3, 4
- [65] Sijie Yan, Yuanjun Xiong, and Dahua Lin. Spatial temporal graph convolutional networks for skeleton-based action recognition. In *AAAI Conference on Artificial Intelligence*, 2018. 2, 6, 7
- [66] Yijun Yang, Zhaohu Xing, Lequan Yu, Chunwang Huang, Huazhu Fu, and Lei Zhu. Vivim: a video vision mamba for medical video segmentation, 2024. 3
- [67] Fanfan Ye, Shiliang Pu, Qiaoyong Zhong, Chao Li, Di Xie, and Huiming Tang. Dynamic gcn: Context-enriched topology learning for skeleton-based action recognition. In *Proceedings of the 28th ACM International Conference on Multimedia*, pages 55–63. ACM, 2020. 2
- [68] Guowen Zhang, Lue Fan, Chenhang He, Zhen Lei, Zhaoxiang Zhang, and Lei Zhang. Voxel mamba: Group-free state space models for point cloud based 3d object detection, 2024. 3
- [69] Jieming Zhang, Jongmin Lim, Moon Hyun Kim, Sungwook Hur, and Tai Myoung Chung. Wm-stgcn: A novel spatiotemporal modeling method for parkinsonian gait recognition. *Sensors*, 23, 2023. 3
- [70] Pengfei Zhang, Cuiling Lan, Wenjun Zeng, Junliang Xing, Jianru Xue, and Nanning Zheng. Semantics-guided neural networks for efficient skeleton-based human action recognition. In *IEEE/CVF International Conference on Computer Vision and Pattern Recognition*, 2020. 7
- [71] Xikun Zhang, Chang Xu, and Dacheng Tao. Context aware graph convolution for skeleton-based action recognition. In *IEEE/CVF International Conference on Computer Vision and Pattern Recognition*, 2020. 2
- [72] Yuhan Zhang, Bo Wu, Wen Li, Lixin Duan, and Chuang Gan. Stst: Spatial-temporal specialized transformer for skeleton-based action recognition. In *ACM International Conference on Multimedia*, pages 3229–3237, 2021. 7
- [73] Zeyu Zhang, Akide Liu, Ian Reid, Richard Hartley, Bohan Zhuang, and Hao Tang. Motion mamba: Efficient and long sequence motion generation, 2024. 3
- [74] Huanyu Zhou, Qingjie Liu, and Yunhong Wang. Learning discriminative representations for skeleton based action recognition. In *IEEE/CVF International Conference on Computer Vision and Pattern Recognition*, 2023. 1, 6, 7, 8
- [75] Yuxuan Zhou, Zhi-Qi Cheng, Chao Li, Yanwen Fang, Yifeng Geng, Xuansong Xie, and Margret Keuper. Hypergraph transformer for skeleton-based action recognition, 2022. 1, 2, 6, 7, 8
- [76] Yuxuan Zhou, Xudong Yan, Zhi-Qi Cheng, Yan Yan, Qi Dai, and Xian-Sheng Hua. Blockgcn: Redefine topology awareness for skeleton-based action recognition. In *IEEE/CVF International Conference on Computer Vision and Pattern Recognition*, 2024. 7
- [77] Anqi Zhu, Qihong Ke, Mingming Gong, and James Bailey. Adaptive local-component-aware graph convolutional network for one-shot skeleton-based action recognition. In *IEEE/CVF Winter Applications of Computer Vision*, 2023. 1